

## Electron-Electron Interaction Effects on the Optical Excitations of Semiconducting Single-Walled Carbon Nanotubes

Hongbo Zhao and Sumit Mazumdar

Department of Physics, University of Arizona, Tucson, Arizona 85721, USA

(Received 7 June 2004; published 5 October 2004)

We report correlated-electron calculations of optically excited states in ten semiconducting single-walled carbon nanotubes with a wide range of diameters. Optical excitation occurs to excitons whose binding energies decrease with increasing nanotube diameter, and are smaller than the binding energy of an isolated strand of poly-(paraphenylene vinylene). The ratio of the energy of the second optical exciton polarized along the nanotube axis to that of the lowest exciton is smaller than the value predicted within single-particle theory. The experimentally observed weak photoluminescence is an intrinsic feature of semiconducting nanotubes.

DOI: 10.1103/PhysRevLett.93.157402

PACS numbers: 78.67.Ch, 71.35.-y, 73.22.-f, 78.55.-m

Recent experiments with semiconducting single-walled carbon nanotubes (SWCNTs) have indicated the strong role of electron-electron ( $e-e$ ) interactions [1–5], ignored in one-electron theories [6]. Several observations have attracted attention. First, optical gaps in SWCNTs are greater [1–3] than those predicted from the tight-binding (TB) model [6]. Second, the ratio of the threshold energy corresponding to the second optical transition polarized along the SWCNT axis to that of the first such transition is less than the value two [2–4] predicted within the TB model for wide SWCNTs [6]. It has been claimed that this “ratio problem” is a signature of  $e-e$  interactions [7]. Third, ultrafast pump-probe spectroscopy has revealed *structured* photoinduced absorptions (PA) and correlations of PA with photoinduced bleaching (PB), that indicate that photoexcitations in SWCNTs are excitons [5]. These observations have led to theoretical studies of SWCNTs that go beyond one-electron models [7–11]. Although a consensus is emerging that optical absorptions in semiconducting SWCNTs are due to excitons, complete physical understanding of the generic effects of  $e-e$  interactions is still missing.

In the present Letter, we investigate SWCNTs within the semiempirical Pariser-Parr-Pople (PPP)  $\pi$ -electron Hamiltonian [12] that has been used extensively to discuss  $\pi$ -conjugated polymers [13–15], which also exhibit strong excitonic features [16,17]. The advantages of the semiempirical approach are that (i) an immediate connection to the rich physics of  $\pi$ -conjugated polymers can be made, and (ii) the dominant effects of  $e-e$  interactions in SWCNTs can be understood physically. Admittedly,  $\pi$ -electron only theory will miss the curvature effects of the narrowest tubes, but our emphasis is on generic conclusions valid also for the widest tubes.

Our work has multiple conclusions. First, we show theoretically that the observed low quantum efficiency (QE) of the photoluminescence (PL) of SWCNTs [4,18–20] is very likely a consequence of the occurrence of optically forbidden exciton states below the optically

allowed exciton. Second, while transverse photoexcitations are not expected to be strongly visible in optical measurements [21], the energetics of these states are nevertheless of interest. While within the TB theory the transverse photoexcitations occur exactly halfway between the two lowest longitudinally polarized absorptions, they are shifted to considerably above the central region. Both these results could have been anticipated from previous work on poly(paraphenylenevinylene) (PPV) [13,15,22]. Third, we show that the “ratio problem” can be understood at the level of mean-field theory of  $e-e$  interactions, and no sophisticated many-body explanation [7] is necessary. Finally, we arrive at generic conclusions about the underlying excitonic electronic structures in ten different SWCNTs with diameters 5.6–13.5 Å.

We consider the PPP model Hamiltonian [12]

$$H = H_{1e} + H_{e-e}, \quad (1a)$$

where  $H_{1e}$  is the one-electron Hückel Hamiltonian and  $H_{e-e}$  is the  $e-e$  interaction,

$$H_{1e} = -t \sum_{\langle ij \rangle, \sigma} c_{i,\sigma}^\dagger c_{j,\sigma} + \text{H.c.}, \quad (1b)$$

$$H_{e-e} = U \sum_i n_{i,\uparrow} n_{i,\downarrow} + \frac{1}{2} \sum_{i,j} V_{ij} (n_i - 1)(n_j - 1). \quad (1c)$$

Here  $c_{i,\sigma}^\dagger$  creates a  $\pi$  electron of spin  $\sigma$  on carbon (C) atom  $i$ ,  $\langle \cdot \cdot \rangle$  denotes nearest neighbors,  $n_i = \sum_\sigma c_{i,\sigma}^\dagger c_{i,\sigma}$  is the total number of  $\pi$  electrons on site  $i$ . The parameters  $t$ ,  $U$ , and  $V_{ij}$  are the nearest-neighbor hopping integral, and the on-site and intersite Coulomb interactions, respectively. We have chosen the standard value of 2.4 eV for  $t$  [13,14]. Our parametrization of the long-range  $V_{ij}$  is similar to the standard Ohno parametrization [23]

$$V_{ij} = \frac{U}{\kappa \sqrt{1 + 0.6117 R_{ij}^2}}, \quad (2)$$

where  $R_{ij}$  is the distance between C atoms  $i$  and  $j$  in Å,

and  $\kappa$  is a screening parameter ( $\kappa = 1$  within Ohno parametrization) [22]. We have done calculations for  $U/t = 1.9, 2.5, 3.33, 4.0$  and  $\kappa = 1$  and 2, and our qualitative conclusions are similar for all cases. We report the results for only  $U/t = 3.33$  and  $\kappa = 2$ , since this combination was found to be the most suitable for PPV [22], and it is likely that the Coulomb parameters in phenyl-based  $\pi$ -conjugated polymers and SWCNTs are similar.

Full many-body calculation within Eq. (1) is not possible for SWCNTs. We use the single configuration interaction (SCI) approximation [13,15,22], which is valid within the subspace of single excitations from the Hartree-Fock (HF) ground state and gives semiquantitative results for one-photon states. We use open boundary condition along the nanotube (NT) axis. Surface states originating from ends of open tubes can be detected from their energies at the chemical potential in the  $U = V_{ij} = 0$  Hückel limit and their one-electron wave functions, and they are excluded from the SCI calculations. We have performed calculations for seven semiconducting zigzag  $(n, 0)$  NTs for  $n$  ranging from 7 to 17, and (6,2), (6,4), and (7,6) chiral NTs. The number of unit cells  $N$  in SCI calculations for zigzag NTs is 18. For the chiral NTs with large unit cells, we determined from Hückel calculations the  $N$  at which infinite system absorption thresholds are reached, and performed the SCI calculations for these  $N$ . Our calculations are for  $N = 10, 8$ , and 2 in the (6,2), (6,4), and (7,6) NTs, with 1040, 1216, and 1016 C atoms, respectively.

We begin our discussions with the lowest energy excitations. In the zigzag SWCNTs the highest valence band (VB) and the lowest conduction band (CB) for  $H_{e-e} = 0$  are doubly degenerate [6]. In the chiral SWCNTs the degenerate levels occur at different single-particle crystal momenta [6]. Nevertheless, in both cases there occur doubly degenerate single-particle excitations with total crystal momentum zero. Consider now the four degenerate lowest single-particle excitations in SWCNTs,  $\chi_{a \rightarrow a'}$ ,  $\chi_{a \rightarrow b'}$ ,  $\chi_{b \rightarrow a'}$ , and  $\chi_{b \rightarrow b'}$ , shown in Fig. 1, where  $a, b(a', b')$  are the highest occupied (lowest unoccupied) one-electron levels. The two excitations  $\chi_{a \rightarrow a'}$  and  $\chi_{b \rightarrow b'}$  are optically allowed, and for nonzero matrix elements of  $H_{e-e}$  between them, new nondegenerate eigenstates  $\chi_{a \rightarrow a'} \pm \chi_{b \rightarrow b'}$  are obtained. There also occur superpositions involving the dipole-forbidden excitations, as well as others involving immediately lower VB and higher CB levels. Significantly, (i) the odd superposition is dipole-forbidden, and (ii) for repulsive  $H_{e-e}$  the allowed even superposition is higher in energy, as is indicated in Fig. 1. In Table I we have given the lowest SCI exciton state energies and the squares of the transition dipole moments between them and the HF ground state, for the two representative cases of (11,0) and (6,2) SWCNTs. In both cases, the exciton state with strong dipole coupling is the highest energy excitation. In the chiral SWCNTs,

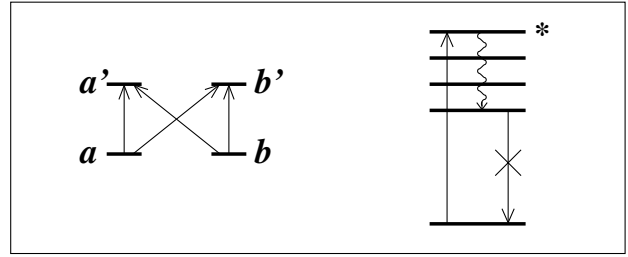


FIG. 1. (Left) Schematic of the four degenerate single-particle excitations from the highest occupied to the lowest unoccupied one-electron levels in SWCNTs. (Right) These degeneracies are split by  $H_{e-e}$ , and only the highest state is strongly dipole allowed. Rapid relaxation occurs to the lowest forbidden exciton, radiative relaxation from which is forbidden.

there occur weakly allowed states in between the strongly allowed state and the lowest exciton state, but the overall behavior is similar. In Table II we have listed  $(n, m)$  for all SWCNTs we have investigated, and the corresponding differences in total energies  $\delta E$  between the optically allowed exciton and the lowest exciton.

The energy spectra of SWCNTs is similar to that of polyacetylenes and polydiacetylenes, where also there occur dipole-forbidden excited states below the optical exciton as a consequence of  $e-e$  interaction [24]. PL is weak in these polymers, as the optically excited state decays in ultrafast times to the low energy dipole-forbidden state, radiative transition from which to the ground state cannot occur. The results of Tables I and II then strongly suggest that the low QE of PL in SWCNTs ( $< 10^{-3}$ ) [4,18–20] is intrinsic. (The one-photon forbidden state in the polymers is two-photon allowed, while the lower energy states in the SWCNTs are not. This difference is of no consequence in emission, which is a one-photon process.) We will return to this issue later.

TABLE I. The energies of the lowest excitons and the squares of the transition dipole couplings between them and the ground state  $G$  (electronic charge  $e = 1$ ). The exciton at energy 1.259 eV in (11,0) is doubly degenerate. Some of the forbidden excitons below the strongly allowed exciton in chiral SWCNTs are odd superpositions of higher energy one-electron excitations.

(11,0)		(6,2)	
$E_i$ (eV)	$ \mu_{G,i} ^2$	$E_i$ (eV)	$ \mu_{G,i} ^2$
1.323	77.4	1.772	95.3
1.321	0	1.768	0
1.259 (2)	0	1.765	0
1.231	0	1.764	13.5
		1.743	0
		1.743	0.327
		1.733	0
		1.710	0

TABLE II. Summary of computed SCI results for different SWCNTs.

$(n,m)$	$d$ (Å)	$\delta E$ (eV)	$E_{b1}$ (eV)	$E_{b2}$ (eV)	$E_{22}/E_{11}$
(7,0)	5.56	0.113	0.540	0.782	1.801
(6,2)	5.72	0.062	0.528	0.718	1.819
(8,0)	6.35	0.098	0.533	0.578	1.646
(6,4)	6.92	0.057	0.480	0.552	1.716
(10,0)	7.94	0.126	0.406	0.574	1.650
(11,0)	8.73	0.092	0.415	0.454	1.726
(7,6)	8.95	0.073	0.365	0.470	1.675
(13,0)	10.3	0.113	0.322	0.454	1.577
(14,0)	11.1	0.089	0.338	0.386	1.677
(17,0)	13.5	0.086	0.288	0.312	1.698

Within TB theory, excitations responsible for optical absorptions polarized transverse to the tube axis,  $\chi_{1\rightarrow 2'}$  and  $\chi_{2\rightarrow 1'}$  (see inset, Fig. 2), are also degenerate. The threshold energy for transverse excitation is exactly half-way between the energies of the two longitudinal excitations  $\chi_{1\rightarrow 1'}$  and  $\chi_{2\rightarrow 2'}$ .  $H_{e-e}$  will also split the degeneracy among the transverse excitations (as mentioned above, we ignore here the depolarization effect [21], as the splitting due to many-body effects will occur independent of the intensity of transverse absorptions). We now expect a dipole-forbidden transition  $\chi_{1\rightarrow 2'}$  -  $\chi_{2\rightarrow 1'}$  shifted below the central region and a dipole-allowed transition  $\chi_{1\rightarrow 2'} + \chi_{2\rightarrow 1'}$  shifted above the central region. In Fig. 2 we have shown the calculated optical absorptions within TB, HF, and SCI approaches for the (8,0) SWCNT. Strong blueshift of the dipole-allowed transverse excitation from the central region is seen. Very similar relative blueshift of the transverse optical excitation has been of strong theoretical [13,15,22] and experimental [13,25] interest in PPV. Detection of this blueshift in SWCNTs can give a measure of the strength of the  $e-e$  interaction.

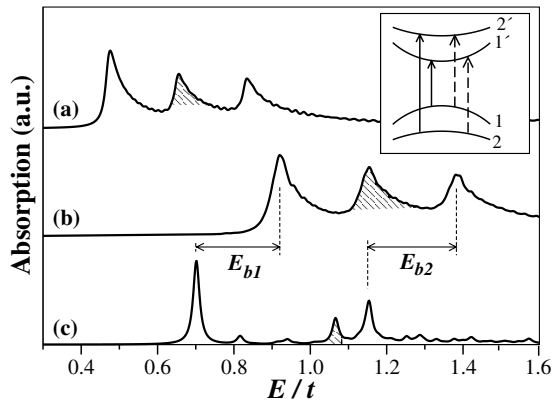


FIG. 2. Absorption spectra of (8,0) nanotube from (a) Hückel, (b) Hartree-Fock, and (c) SCI calculations. Shaded peaks indicate transverse polarized absorptions. The inset shows longitudinal (solid arrows) and transverse (dashed arrows) excitations.

We now focus on the longitudinal absorptions. Our calculated spectra in all cases resemble the three spectra in Fig. 2 for the (8,0) NT. Within SCI the HF thresholds are the edges of the continuum bands corresponding to each class of excitations. Thus, in Fig. 2,  $E_{b1}$  and  $E_{b2}$  are the binding energies of the two lowest excitons. We examine  $E_{22}/E_{11}$ , where  $E_{11}$  and  $E_{22}$  are the energies of the two lowest longitudinal absorptions. The TB  $E_{22}/E_{11}$  is close to 2 for the (8,0) NT, but even at the HF level  $E_{22}/E_{11} < 2$ . Unless the correlation-induced blueshift of  $E_{22}$  is twice that of the  $E_{11}$ , the ratio is bound to be less than 2. The energy shifts are nearly the same for both absorption features at both HF and SCI levels, for all the SWCNTs that we have investigated. As shown in Table II the SCI  $E_{22}/E_{11}$  for large diameter NTs is close to the experimental value of  $\sim 1.7$  [4].

Each exciton in the SWCNTs has its own binding energy, as shown in Fig. 2 for the (8,0) NT. In Table II we have listed the exciton binding energies  $E_{b1}$  and  $E_{b2}$  for different SWCNTs. For the narrowest NTs,  $E_{b2} > E_{b1}$ , while for the widest NTs  $E_{b2} \approx E_{b1}$ . The general features of (i) decreasing  $E_{b1}$  and  $E_{b2}$  with increasing diameter  $d$ , (ii)  $E_{b2} > E_{b1}$  for the narrowest NTs, and (iii)  $E_{b2} \approx E_{b1}$  in the widest NTs are true for all  $U$  and  $\kappa$ .

In Ref. [22] we had shown that the combination  $U = 8.0$  eV and  $\kappa = 2$  (out of a total of 15 sets) gave the best fits to four different absorption bands in PPV, and that with this parameter set the calculated exciton binding energy is  $\sim 0.9 \pm 0.2$  eV. Very similar magnitude was subsequently calculated within an *ab initio* approach that included solution of the Bethe-Salpeter equation for the two-particle Green's function [26]. Using the same  $U$  and  $\kappa$  we find that the  $E_{b1}$  in the widest SWCNTs in Table II are about 0.3 eV, while in the narrower NTs  $E_{b1} \sim 0.5$  eV. Indeed, for all eight combinations of  $U$  and  $\kappa$  we found that the exciton binding energies in the SWCNTs are smaller than in PPV. Conwell has suggested that the exciton binding energy in PPV should be redefined as the energy required to dissociate the exciton into a pair of oppositely charged polarons, and that taking into account the relaxation energy of the polarons one obtains exciton binding energy 0.4 eV in PPV [27]. Further work is required to determine whether such a correction is appropriate for SWCNTs.

In Fig. 3 we have plotted the calculated SCI  $E_{11}$  and  $E_{22}$  for all ten SWCNTs against their inverse diameters  $1/d$ . The linear decrease of the optical excitation energies with decreasing  $1/d$ , observed experimentally, is well reproduced. The absolute energies are larger than what are experimentally observed, as expected, as SCI is not entirely a quantitative method. This can also indicate that  $e-e$  interactions in the SWCNTs are somewhat smaller.

We now return to our conclusion that the low QE of PL ( $< 10^{-3}$ ) [4,18–20] in SWCNTs is an intrinsic feature of isolated NTs. As shown in Table II,  $\delta E \sim (3-4)k_B T$ . Thus following the rapid relaxation into the forbidden lowest

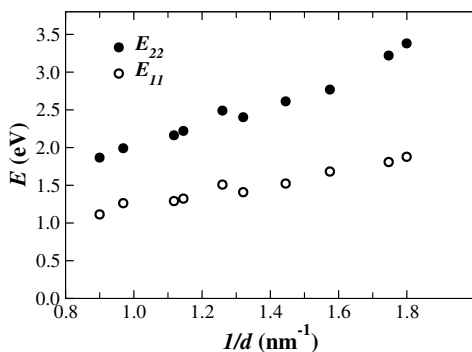


FIG. 3. Calculated energies of the two lowest excitons vs inverse diameter of the SWCNTs.

exciton it is unlikely that thermal effects will reexcite the system to the allowed state. Intrinsic radiative decay rate therefore should be low, and the radiative lifetimes large. Simultaneously,  $\delta E$  is small enough that small amounts of impurities or changes in the environment can modify the emissive behavior. This may explain the strong dependence of the emission on the environment [4,18,19,28]. Recent estimates of very long exciton lifetimes [19,20] are in agreement with our work. Femtosecond time-resolved measurements indicate same decay rates for fluorescence and PB, but the PB drops to only half its peak value [19]. We agree with Ref. [19] that this is an indication of trapping of the excitation in a nonemissive state. We also believe that the nonemissive state is the forbidden exciton found here.

In summary, semiempirical configuration interaction calculations reveal excitonic electronic structures for SWCNTs. Corresponding to each band-to-band transition within TB theory, there occurs an optical exciton in SWCNTs. The ratio problem is a simple consequence of nearly equal blueshifts of the two lowest optical absorptions from their TB frequencies. The binding energies of the lowest two excitons decrease with increasing diameter and the two binding energies are comparable for wide NTs. Assumption of similar Coulomb parameters in SWCNTs and phenyl-based  $\pi$ -conjugated polymers gives smaller binding energy for the former. We estimate 0.3–0.5 eV binding energy for the wide SWCNTs. We ascribe the low QE of the PL in SWCNTs to the occurrence of optically forbidden excitons below the optical exciton, which in turn is a consequence of the splitting of the degeneracy that exists in the one-electron limit by  $e$ - $e$  interactions. A similar degeneracy splitting should also occur between the states to which optical excitations transverse to the NT axis occurs.

This work was supported by NSF-DMR-0406604, NSF-ECS-0108696, and the NSF STC at the University of Arizona. We acknowledge useful discussions with Professor Yu. N. Gartstein, Professor E. J. Mele, and Professor Z. V. Vardeny.

*Note added.*—Forbidden excitons below the lowest optical exciton in zigzag SWCNTs have been discussed

recently [29]. Recent work has also claimed that the origin of the ratio problem is the Coulomb self-energy [30], in agreement with the work presented here.

- 
- [1] M. Ichida *et al.*, Phys. Rev. B **65**, 241407 (2002).
  - [2] X. Liu *et al.*, Phys. Rev. B **66**, 045411 (2002).
  - [3] S. M. Bachilo *et al.*, Science **298**, 2361 (2002).
  - [4] M. J. O'Connell *et al.*, Science **297**, 593 (2002).
  - [5] O. J. Korovyanko *et al.*, Phys. Rev. Lett. **92**, 017403 (2004).
  - [6] R. Saito, G. Dresselhaus, and M. S. Dresselhaus, *Physical Properties of Carbon Nanotubes* (Imperial College Press, London, 1998).
  - [7] C. L. Kane and E. J. Mele, Phys. Rev. Lett. **90**, 207401 (2003).
  - [8] T. Ando, J. Phys. Soc. Jpn. **66**, 1066 (1997).
  - [9] M. F. Lin, Phys. Rev. B **62**, 13153 (2000).
  - [10] C. D. Spataru *et al.*, Phys. Rev. Lett. **92**, 077402 (2004).
  - [11] E. Chang *et al.*, Phys. Rev. Lett. **92**, 196401 (2004).
  - [12] R. Pariser and R. G. Parr, J. Chem. Phys. **21**, 466 (1953); J. A. Pople, Trans. Faraday Soc. **49**, 1375 (1953).
  - [13] M. Chandross *et al.*, Phys. Rev. B **50**, 14702 (1994); **55**, 1486 (1997); **59**, 4822 (1999).
  - [14] P. C. M. McWilliams, G. W. Hayden, and Z. G. Soos, Phys. Rev. B **43**, 9777 (1991); A. Race, W. Barford, and R. J. Bursill, *ibid.* **64**, 035208 (2001); S. Ramasesha *et al.*, Adv. Quantum Chem. **38**, 121 (2000), and references therein.
  - [15] M. J. Rice and Yu. N. Gartstein, Phys. Rev. Lett. **73**, 2504 (1994).
  - [16] J. M. Leng *et al.*, Phys. Rev. Lett. **72**, 156 (1994); S. V. Frolov *et al.*, *ibid.* **85**, 2196 (2000).
  - [17] G. Weiser, Phys. Rev. B **45**, 14076 (1982); D. Guo *et al.*, *ibid.* **48**, 1433 (1993); M. Liess *et al.*, *ibid.* **56**, 15712 (1997).
  - [18] S. Lebedkin *et al.*, J. Phys. Chem. B **107**, 1949 (2003).
  - [19] F. Wang *et al.*, Phys. Rev. Lett. **92**, 177401 (2004).
  - [20] C.-X. Sheng, Z. V. Vardeny, A. B. Dalton, and R. H. Baughman (unpublished).
  - [21] H. Ajiki and T. Ando, Physica (Amsterdam) **201B**, 349 (1994).
  - [22] M. Chandross and S. Mazumdar, Phys. Rev. B **55**, 1497 (1997).
  - [23] K. Ohno, Theor. Chim. Acta **2**, 219 (1964).
  - [24] B. S. Hudson *et al.*, in *Excited States*, edited by E. C. Lim (Academic Press, New York, 1982).
  - [25] D. Comoretto *et al.* Chem. Phys. Lett. **289**, 1 (1998).
  - [26] M. Rohlfing and S. G. Louie, Phys. Rev. Lett. **82**, 1959 (1999).
  - [27] E. M. Conwell, in *Organic Electronic Materials*, edited by R. Farchioni and G. Grosso (Springer-Verlag, Berlin, 2001), pp. 127–180.
  - [28] J. Lefebvre, Y. Homma, and P. Finnie, Phys. Rev. Lett. **90**, 217401 (1999).
  - [29] V. Perebeinos, J. Tersoff, and P. Avouris, Phys. Rev. Lett. **92**, 257402 (2004).
  - [30] C. L. Kane and E. J. Mele, cond-mat/0403153.